Ground Resistance of Buried Metallic Parts in Urban Areas: an Extensive Measurement Campaign

Ground Resistance of Buried Metallic Parts in Urban Areas: an Extensive Measurement Campaign

Giuseppe Cafaro *, Pietro Colella ‡, Pasquale Montegiglio *,
Enrico Pons ‡, Riccardo Tommasini ‡, Francesco Torelli *, Giovanni Valtorta †
* DEI, Politecnico di Bari, Bari, 70126, Italy, Email: pasquale.montegiglio@poliba.it
‡ DENERG, Politecnico di Torino, Torino, 10129, Italy, Email: pietro.colella@polito.it
† e-distribuzione SpA, Roma, 00198, Italy, Email: giovanni.valtorta@e-distribuzione.com

***Abstract*—In urban and industrial areas, a relevant presence of buried metallic objects (e.g. gas and water pipes, etc.) can be detected. Usually, these elements are imagined as widespread, meshed metallic grids in a good contact with the soil. In the last years, an arising interest on their role in the identification of a Global Earthing System (GES) has been expressed by the scientific community. Unfortunately, the geometrical and electrical properties of this kind of buried metallic parts cannot be provided by any documentations. This is mostly due to the fact that no trustworthy schemes are provided, as the management of these metallic parts is responsibility of different companies, which have installed them during several years. In order to characterize the buried metallic elements with reference to the electrical safety issue, the main quantity of interest is their resistance to earth. With this aim, a field measurement campaign was organized and the resistance to earth of more than 800 metallic objects has been evaluated through a simplified measurement protocol. In this paper, the measurement protocol, the set-up, the results and their analysis are reported.**

***Index Terms*—Earthing system; extraneous-conductive-part; global earthing system; ground resistance; grounding electrodes; indirect contacts; MV distribution faults; power distribution faults; resistance measurement; resistance to earth.**

I. Introduction

MV distribution systems in densely populated areas, such as residential and industrial zones, normally consist of a large number of MV/LV substations which are close to each other and interconnected (at least) through MV cables sheaths [1].

This tight interconnection of earthing systems (ESs) makes for an overall grounding network, which may cover large areas. In case of a single line to ground fault (SLGF), this provides two main effects:

- a distribution of the fault current between the grounding electrode of the faulty substation and the interconnected installations (neighbouring MV/LV substations, water/gas pipeline, etc.) [1], [2], [3], [4], [5];
- a smoothing of the Earth Potential Profile (EPR), reducing the hazardous voltage gradients [6], [7], [8].

What previously mentioned is the basis for the Global Earthing System (GES) definition provided by the International Standards IEC EN 61936-1 and EN 50522: *"equivalent earthing system created by the interconnection of local earthing systems that ensures, by the proximity of the earthing systems, that there are no dangerous touch voltages"* [9] [10] [11].

Even if the physical phenomena related to the GES definition are now almost clear, no official practical guidelines are given in any standard yet. Although the evaluation of specific cases is feasible, a general procedure to identify GESs, based on both simple and operative rules, is difficult to achieve [12], [13], [14], [15], [16], [17].

As proved in previous works, the GES effects can be enhanced by other several metallic parts (commonly widespread in city centers, urban or industrial areas), such as LV ESs, water/gas pipelines, railway and tramway tracks, if interconnected to the MV earthing network [7], [18].

Cases of interconnection among ESs and Extraneous Conductive Parts (ExCPs), e.g. water and gas pipes, can especially be found in industrial and urban contexts. For example, in the case of a MV user with a private MV/LV substation (industrial area), the ES of the substation and the ExCPs shall be interconnected to create the protective equipotential bonding [19]. The earthing system, in turn, shall be interconnected with the MV earthing grid through the MV cable sheaths. Another example of interconnection occurs when a MV/LV substation (owned by the DSO) and LV users are located in a same reinforced concrete building. This scenario is quite common in Italian urban areas. According to the IEC 60364-4, the extraneous conductive parts (such as gas and water pipes) and the metallic reinforcements of constructional reinforced concrete shall be interconnected to the LV main earthing terminal [19]. At the same time, according to EN 50522, the metallic reinforcements could be interconnected to the main earthing terminal of the MV/LV substation [10]. In this way, the MV earthing network and the extraneous conductive parts would be galvanically interconnected.

Unfortunately, the geometrical and electrical properties of buried metallic parts are not available, as well as information about their interconnection level with the MV ESs. Moreover, no trustworthy schemes reporting this information can be provided, because the management of these metallic parts is responsibility of different companies, which have installed them during several years. To characterize the buried metallic elements, one of the main quantity of interest is their resistance to earth, which is the synthetic parameter that allows their

This paper was developed as part of the research "METERGLOB" co-funded by the CCSE (today CSEA, Cassa per i Servizi Energetici e Ambientali) with the participation of six partners: Enel Distribuzione, Istituto Italiano del Marchio di Qualitá IMQ, Politecnico di Bari, Politecnico di Torino, Universitá di Palermo and Sapienza Universitá di Roma.

global behavior estimation in terms of electrical safety. For these reasons, a field measurement campaign was organized to evaluate their resistance to earth and their interconnection level to the MV earthing network. A simplified measurement protocol has been applied to more than 800 metallic objects by Enel Distribuzione, the main Italian Distribution System Operator (DSO), as shown in a previous work of the author [20]. In this paper, the adopted experimental setup and the measurement results are shown. Furthermore, a statistical analysis is presented, considering the influence of the soil resistivity and the types of neighborhood (old town city center, recently built neighborhood and suburbs).

II. Measurement Campaign

In this section, the measuring circuit and the criteria adopted for the selection of the measurement sites are described,

A. Measurement setup

The main goal of this paper is the characterization of metallic parts buried in urban areas where a GES may exist. For this purpose, the resistance to earth of light poles, gas and water pipes, fire hydrants, fences and similar elements has been measured during the campaign. Due to the large number of tests conducted (more than 800) a simplified methodology was adopted, which required the subsequent calculation of the quantity of interest. The measuring setup is depicted in Fig. 1. Briefly, the earthing system of the MV/LV substation and the buried conductor under test was connected to a variable auto-transformer (VARIAC), which controlled the circulating current. The impedance Z_S of the loop created by the resistance to earth of the MV/LV substation earthing system R_{ES} and the resistance to earth of the generic buried conductor under test R_{BC} was then measured. For safety reasons the flowing current I_F was kept below 5 A. The two-wires impedance measurement procedure was adopted, adequately taking into consideration the interconnecting conductor impedance Z_{IC}.

Since the imaginary part of Z_S is significantly lower than the real one, in this paper only $R_S = Re\{Z_S\}$ is taken into account.

The resistance to earth R_{ES} is a known value, periodically measured by the DSO. By subtracting it from R_S, an assessment of the resistance to earth of the buried conductor R_{BC} can be obtained with an approximation that depends on the R_{ES} uncertainty and on the interference level between the two electrodes. The problem of the interference will be addressed and discussed in Section III.

B. Sample selection

For the execution of the tests reported in this paper, measurement sites were selected in several Italian municipalities. Fig. 2 shows the involved areas and the number of tests carried out in each location. As typical cases of GES are in city centers, urban or industrial areas [10], municipalities characterized by having, at least, a population density of 500 inhabitants per square kilometer were selected. Where possible, in order to cover each typical urban scenario, the

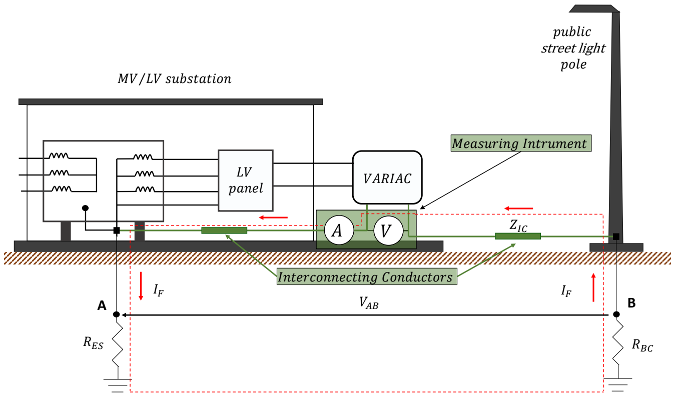

Figure 1. Measuring setup.

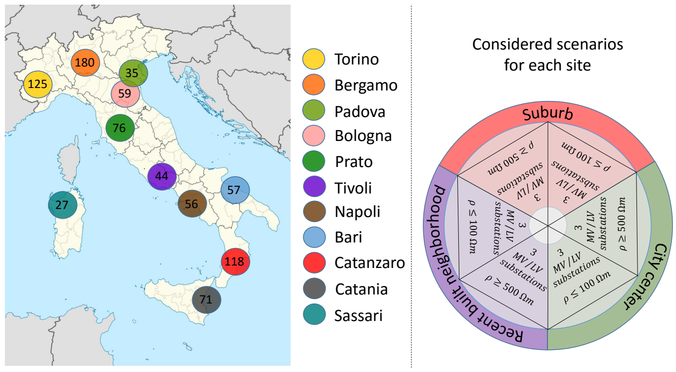

Figure 2. On the left, measurement sites: values represent the number of tests carried out in the relative location; on the right, the characteristics of the 18 MV/LV substations considered for each site.

choice of the MV/LV substations was oriented on sites located within:

1) city centers;
2) suburbs;
3) recently built neighborhood (built up in the last 5 years).

Sites characterized by different soil resistivity were chosen, in order to get a sample as varied as possible.

Fig. 2 summarizes, for each measurement site, the properties of the considered urban contexts where MV/LV substations are located.

The absence of significant electromagnetic disturbance sources (e.g. antennas, close overhead lines, etc.) was also preliminary verified.

III. Interference Phenomenon: A Theoretical Point of View

The adopted simplified measurement methodology allows the assessment of the R_{BC} value with a certain approximation. Not considering the uncertainty on R_{ES}, the measured value reflects the true earth resistance of the buried conductor only if the interference phenomenon with the ES of the MV/LV substation can be neglected. In this section, a short summary of this interaction is presented.

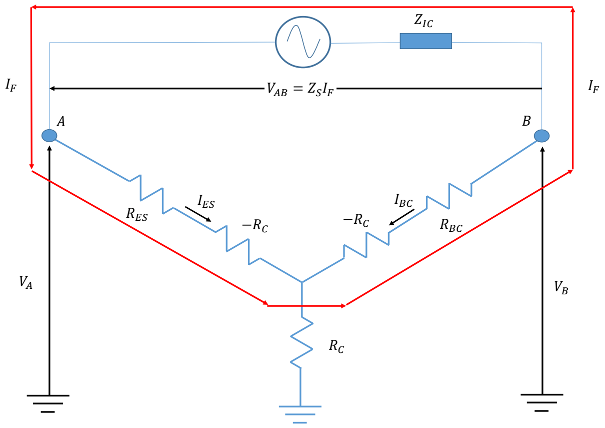

Figure 3. Interference phenomenon equivalent circuit.

As known in literature [7], [21], [22], the interference phenomenon between two electrodes buried in the soil can be represented, in *quasi-static* condition ($50Hz$), by pure resistive parameters. The star of connected resistors reported in Fig. 3 (solid blue line) arises from the linear system 1 by adding and subtracting the quantities $R_C I_{ES}$ and $R_C I_{BC}$ in the first and in the second equation respectively:

$$\begin{cases} V_A = R_{ES} I_{ES} + R_C I_{BC} \\ V_B = R_C I_{ES} + R_{BC} I_{BC} \end{cases} \tag{1}$$

With reference to the typical test case considered for this work:

- R_{ES} is the equivalent resistance of the entire grounding network made up by the interconnected ESs of the MV/LV substations. It may also include the LV neutral *reinforcement groundings* [18];
- R_{BC} is the earth resistance of the metallic part under test. Depending on the effectiveness of its contact with the ground, its extension and electrical continuity, R_{BC} may assume low values ($\leq 1\ \Omega$);
- I_{ES} and I_{BC} are the currents flowing through R_{ES} and R_{BC} respectively;
- R_C is the *mutual transfer resistance*. It can be considered as the transferred voltage on the "passive" grounding electrode when the "active" one is leaking a unitary current [21] and it is defined as follows:

$$R_C = \alpha R_{ES} = \beta R_{BC} \tag{2}$$

where

$$\alpha = \left.\frac{V_B}{V_A}\right|_{I_{BC}=0} < 1; \quad \beta = \left.\frac{V_A}{V_B}\right|_{I_{ES}=0} < 1 \tag{3}$$

The stronger is the interference phenomenon, the larger are coefficients α and β.

According to eq. (2) and eq. (3), R_C is always lower than the smallest between R_{ES} and R_{BC}:

$$R_C < \min\{R_{ES}, R_{BC}\} \tag{4}$$

The series resistance R_S, measured in the test, can be analytically expressed as follows:

$$R_S = R_{ES} + R_{BC} - 2R_C \tag{5}$$

Subtracting R_{ES} from R_S, the resistance to earth of the buried conductor R_{BC} can be computed, save for $2R_C$.

The lower is the interference phenomenon, the lower is the resistance R_C.

IV. Measurement Results

The total number of measurements is reported in Table I. In the second column, their distribution with reference to the metal object type is also shown. The third column reports the number of cases where it was not possible to inject a current greater than 1 A without increasing the voltage level over the safety limit (50 V). For the particular case of light poles, this can be due to the fact that, in the installation phase, concrete is usually poured with a plastic pipe to preserve the hole for the pole installation. If the plastic pipe used as a mould is not removed, the result is that the pole will be isolated from ground. In the case of pipelines, instead, this is probably due to the increasing adoption of non metallic pipes in the water (and gas) distribution networks. From the forth column it can be noticed that a number of 44 abnormal data (unstable output of the instrument) was discarded.

In Fig. 4, the cumulative distribution function (CDF) of R_S for all the buried metallic objects is reported. This representation allows for an immediate evaluation of the acquired data distribution. Fig. 4 clearly shows that the measured R_S is lower than 20 Ω for more than the 80% of all the samples.

However, just the 20% is significantly lower than 1Ω. Considering the minimum cross-sections of earthing conductors required by EN 50522 (copper 16 mm^2, aluminium 35 mm^2, steel 50 mm^2), in the worst case, a galvanic interconnection of about $1km$ length should be provided to obtain an R_S equal to 1 Ω. As the measurements were all carried out in a 100 m radius area around the considered substations, it can be reasonably concluded that the MV ESs and the buried metallic parts are disconnected in the 80% of the cases. A galvanic interconnection established by a smaller cross-section cable could result in the measured R_S; this case is not taken into account because the resulting connection could not be considered stable in time, not fulfilling the mechanical and stability requirements against corrosion.

In Fig. 5, the CDF of the MV/LV substations resistance to earth, R_{ES}, measured by the DSO, is reported. With few exceptions, the measured values are extremely low: the

Table I
Number of Measurements

Buried conductor type	Total	High earth resistance	Discarded
Light Poles	204	36	9
Gas Pipelines	107	11	3
H_2O Pipelines	112	32	10
Other	415	126	22
TOTAL	**838**	**205**	**44**

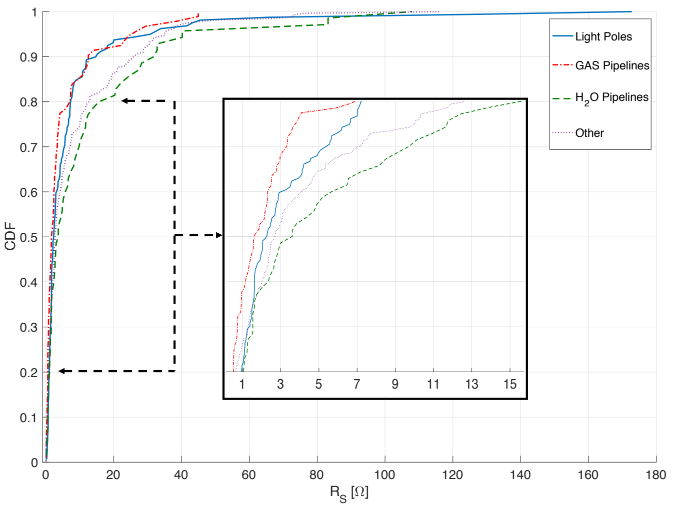

Figure 4. Cumulative distribution function (CDF) of R_S for all the metallic buried parts.

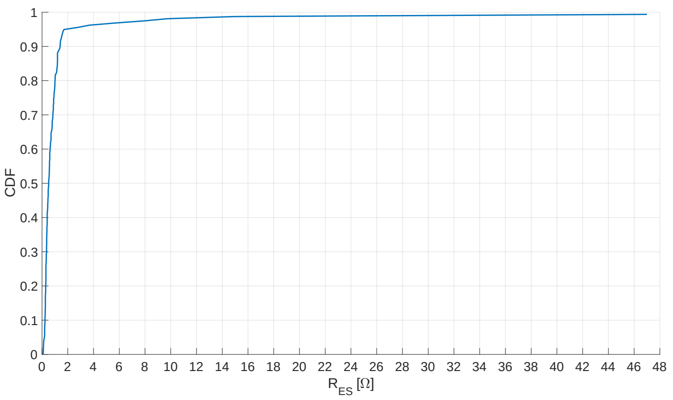

Figure 5. Cumulative distribution function (CDF) of the earth resistance R_{ES} of the MV/LV substations involved in the measuring campaign.

mean value is lower than 1Ω, which is typical of the overall distribution grounding network equivalent resistance.

As shown in the previous section, subtracting from R_S the resistance to earth of the MV/LV substation earthing system, the following quantity can be evaluated:

$$R^*_{BC} = R_{BC} - 2R_C \tag{6}$$

It must be highlighted that R_{ES} and R_S were not measured simultaneously. For this reason, the computation of R^*_{BC} is affected by an additional measurement error. In fact, due to the weather conditions, the resistivity of the upper layer soil could fluctuate during the year [23], [24], [25], with a consequent effect on the value of the earth resistance. However, this error is not significant because MV/LV substation ESs are typically formed by both horizontal and vertical electrodes, as suggested by the IEEE Standard 80 to compensate this fluctuation. The role of vertical rods is to stabilize the performance of the grounding system by reaching lower soil layers, where the resistivity remains nearly constant [26]. Moreover, as

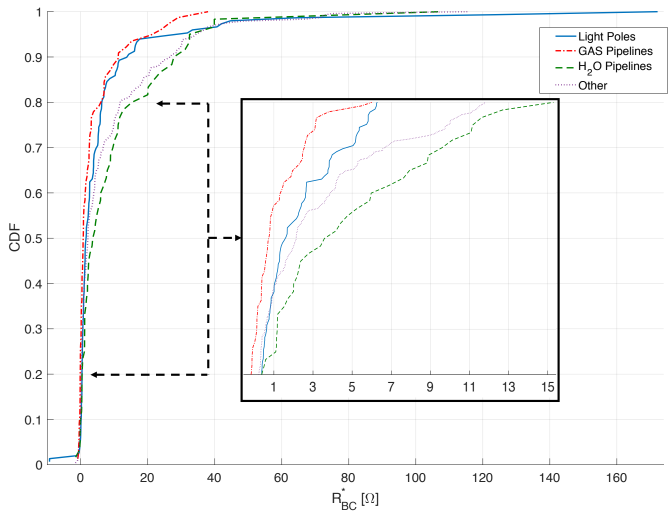

Figure 6. Cumulative distribution function (CDF) of R^*_{BC} for all the metallic buried parts.

previously mentioned, R_{ES} can be generally considered as the equivalent resistance to earth of the MV earthing grid. The variation of the performance of a single earthing system is then mitigated even more.

In Fig. 6, the CDF of R^*_{BC} is depicted with reference to all buried metallic parts.

The analysis of Fig. 6 shows negative R^*_{BC} for same cases: according to eq. (6), this occurs when $2R_C > R_{BC}$, that is when there is a strong interference phenomenon and the values R_{ES} and R_{BC} are comparable.

For each urban scenario, the minimum and the maximum of R^*_{BC} are shown in Fig. 7. The lines between vertical bars intercept the relative mean values. Below each scenario, the number of measurements is also reported. It was not possible to evaluate R^*_{BC} for all the cases since, for a small number of MV/LV substations, R_{ES} was not available.

Moreover, it can be observed that the R^*_{BC} mean values are similar, independently of both the buried conductor type and the urban scenarios.

For all the cases, the minimum and mean values of R^*_{BC} are close each other. This means that the highest values refer to a very limited set of samples.

The resistance to earth of an electrode depends on its geometry and on the soil resistivity. Since the measurements were all carried out in a 100 m radius area around the considered substation, in first approximation it is reasonable to consider both the electrodes buried in a soil with the same properties. So, to decouple measurements from the resistivity parameter [18], the coefficient K was defined as:

$$K = \frac{R_S}{R_{ES}} \tag{7}$$

Fig. 8 shows K values, grouped with reference to scenarios. It was not possible to evaluate K for all the cases since, for a small number of MV/LV substations, R_{ES} was not available. As the R_{ES} values are comparable for the most considered

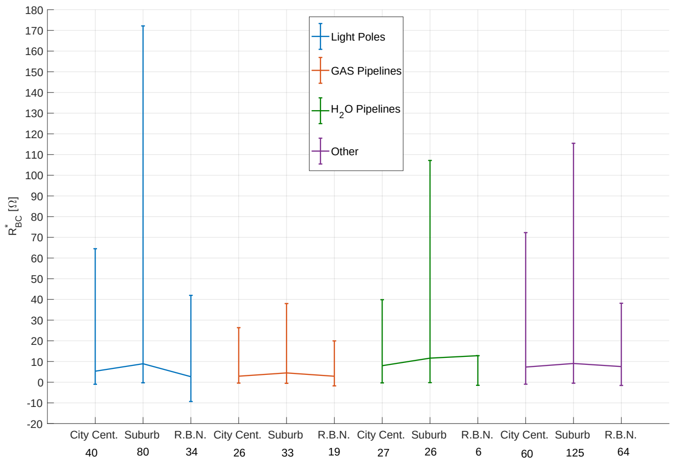

Figure 7. R^*_{BC} measurements (minimum, mean and maximum value) for each urban scenario (City Centers, Suburbs, Recently Built Neighborhoods).

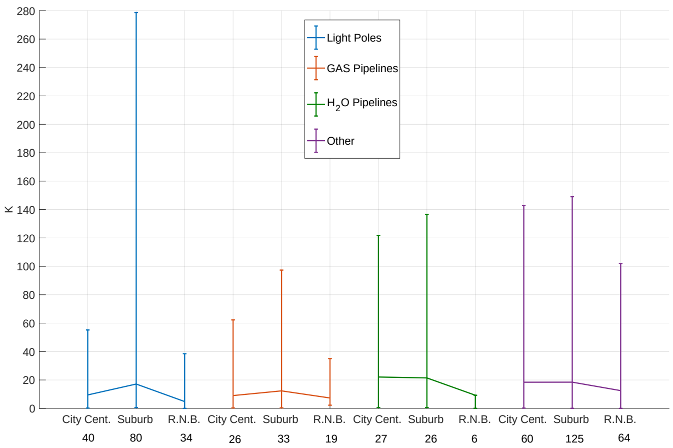

Figure 8. K values (minimum, mean and maximum) for each urban scenario (City Centers, Suburbs, Recently Built Neighborhoods).

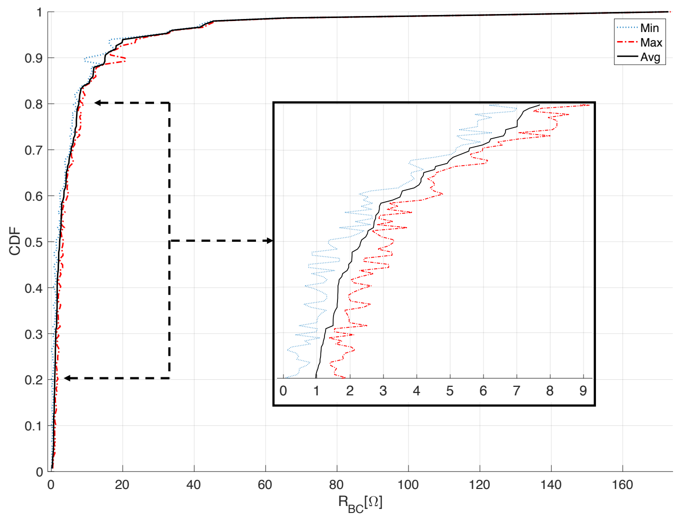

Figure 9. Light poles: cumulative distribution function (CDF) of the average value of R_{BC}. For each point, the theoretical minimum and maximum values of R_{BC} are shown.

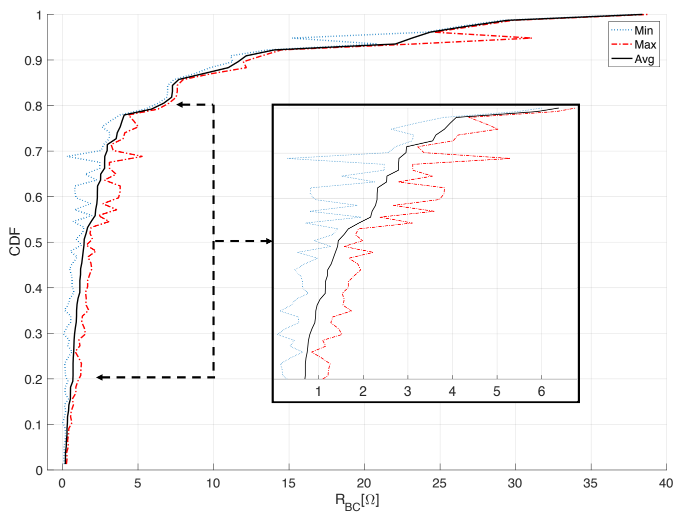

Figure 10. GAS pipelines: cumulative distribution function (CDF) of the average value of R_{BC}. For each point, the theoretical minimum and maximum values of R_{BC} are shown.

substations (with reference to Fig. 5), Fig. 8 is representative of the R^*_{BC}.

The same conclusions given for Fig. 7 are generally valid for K minimum, mean and maximum values. This suggests that the large extension of metallic objects plays a predominant role against the soil resistivity.

Moreover, as shown in appendix VI-B, by the knowledge of K and R_{ES}, it is possible to evaluate the maximum and minimum theoretical values of R_{BC}, which are reported, for all the samples, in Fig. 9 - 11 along with their average value.

The analysis of the curves shows that, for all the considered cases, the variability interval of R_{BC} is quite narrow.

Moreover, Fig. 12 - Fig. 14 show the minimum R_{BC} and the measured R^*_{BC}.

The distance among the curves is quite short for all the considered buried conductors. In accordance to (6), this means that R_C must be small with reference to R_{BC} for the most cases (i.e. the interference phenomenon has not a statistically significant role in the evaluation of R_{BC}).

According to this, the measurement procedure presented in this work statistically allows for a good evaluation of the resistance to earth of a buried metallic part.

The obtained average earth resistance value is particularly important in order to rethink the effectiveness of structural earth electrodes [10]. Especially some Extraneous Conductive Parts (ExCPs), such as water and gas pipes, are generally imagined as widespread meshed metallic earthing networks thanks to their own extent and to their interconnections with local LV and MV ESs (protective equipotential bonding). As a consequence, their resistance to earth is imagined to be extremely low, providing a great contribution in injecting a fault current into the ground. The mean value of the resistance to earth resulting from the reported measurement campaign suggests that the extent and the interconnection level of this

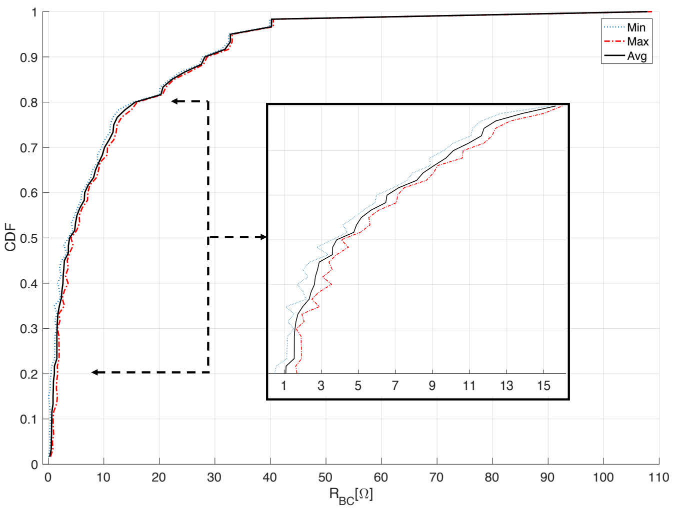

Figure 11. Water pipelines: cumulative distribution function (CDF) of the average value of R_{BC}. For each point, the theoretical minimum and maximum values of R_{BC} are shown.

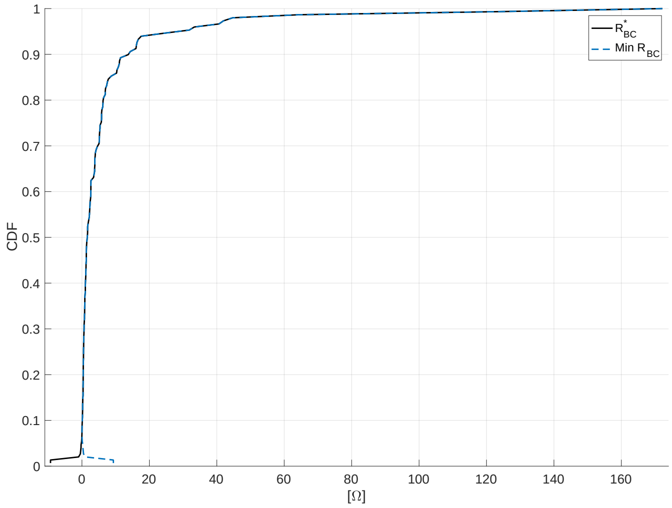

Figure 12. Light poles: comparison between cumulative distribution function (CDF) of the measured $R_{BC}*$ and the theoretical minimum of R_{BC}.

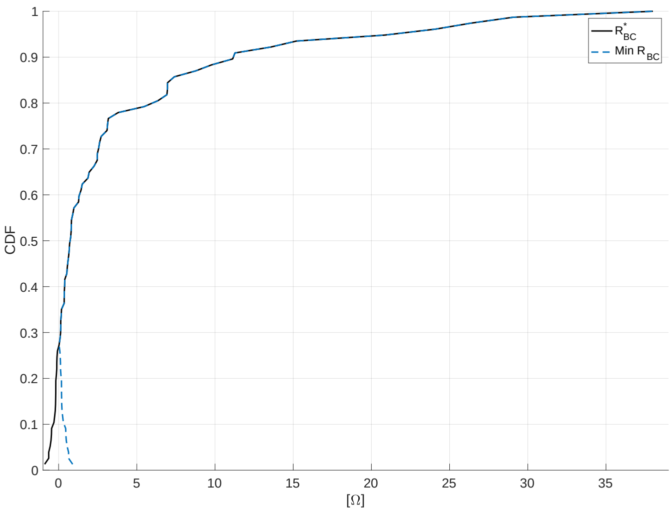

Figure 13. GAS pipelines: comparison between cumulative distribution function (CDF) of the measured $R_{BC}*$ and the theoretical minimum of R_{BC}.

earthing network should be reconsidered. As a comparison, for a soil characterized by a medium resistivity (100 Ωm), the same resistance to earth can be obtained by an ES formed by ten interconnected earthing rods with a length of 1 m, which is quite different from the above mentioned widespread meshed configuration. In conclusion, even if ExCPs improve the effectiveness of an ES, their contribution is not so relevant to be considered a key factor in GES safety and certification. On the contrary, due to their extent, they can introduce an electric potential in the area around the substation. For this reason, people can be exposed to dangerous touch voltages. In order to limit the risk of electric shock as much as possible, it is important to properly choose the metallic objects that should be interconnected. It is a common practice to bond all the metallic elements being within the substation to the local ES. Only Exposed Conductive Parts (ECPs) and ExCPs should be bonded instead [10]. Every metallic object that cannot be classified as an ECP or ExCP (i.d. it cannot introduce a remote electric potential), such as small metallic grid, metallic doors, conductive fences having a small extent, etc., shall not be interconnected. This is important in order to avoid that, in case of fault, the EPR would be accessible from the substation outside. As an example, the person in contact with both the substation door and a nearby metallic object (such as a water pipe or lighting pole, etc.) will be subjected to a higher touch voltage in case of door-substation ES interconnection. Vice-versa, if a door is an ECP (e.g. because it is electrically driven), the nearby metallic object shall be interconnected to the substation ES; in fact, it should be considered as an ExCP, able to introduce an electric potential in the area.

V. Conclusion

The total number of data collected by the measurements campaign is 838. Not considering the discarded 44 abnormal values (unstable output of the instrument), about 25% of the buried conductors present a very high value of resistance to earth.

For the 587 remaining buried conductors (about 70% of the total number of collected data), independently of the type and of the urban scenarios, an average earth resistance value of 10Ω can be considered.

In order to decouple measurements from the resistivity parameter, the ratio K between the measured resistance R_S and the resistance to earth of the MV/LV substation ES was computed. Also in this case, no significant differences can be noticed with reference to both the type of buried conductors and the urban scenario.

The R_{BC} mean value resulting from the reported measurement campaign (about 10 Ω) suggests that the extent, the effectiveness of the contact with the soil, and the interconnection level of metallic objects buried in urban scenarios are

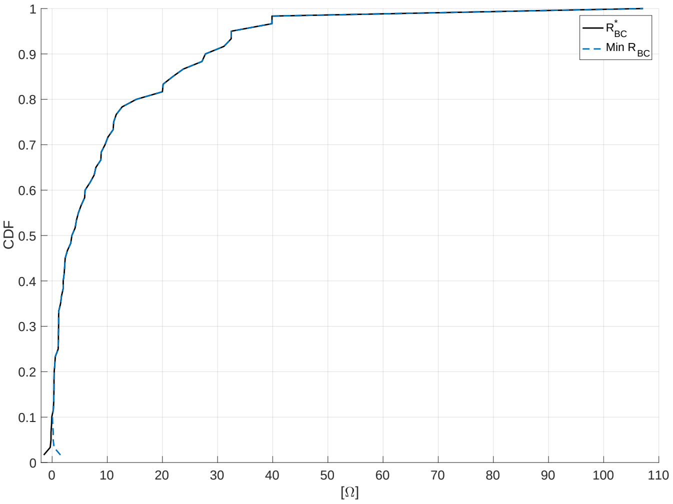

Figure 14. Water pipelines: comparison between cumulative distribution function (CDF) of the measured $R_{BC}*$ and the theoretical minimum of R_{BC}.

generally lower than expected, thus reducing the relevance of their contribution to the safety of a GES.

For the measurements analyzed, the interference phenomenon has not a statistically significant role in the evaluation of R_{BC}.

Therefore, the measurement procedure allows for a good evaluation of the resistance to earth of a buried metallic part, without resorting to the traditional three- or four-wires impedance measurement protocols. As an example, the presented methodology can be particularly useful in order to evaluate the protection against indirect contacts for a public lighting system, expecially in an urban context. The adopted method does not require positioning the auxiliary current electrode and the voltage probe at great distances from the ES under test, which can be quite difficult in urban areas.

VI. Appendix

A. K Analitical Expression

Dividing both sides of (5) by R_{ES} and considering that $R_C = \beta R_{BC}$, it is possible to write the K coefficient expression as a function of β and the ratio R_{BC} / R_{ES}:

$$K = \frac{R_S}{R_{ES}} = 1 + (1 - 2\beta)\,\frac{R_{BC}}{R_{ES}} \tag{8}$$

B. Maximum and minimum values of R_{BC}

From the equation (8) it is possible to write β coefficient as a function of K:

$$\beta = \frac{1}{2}\left(1 - \frac{(K-1)\,R_{ES}}{R_{BC}}\right) \tag{9}$$

With reference to (3), it is here recalled that coefficient β represents the portion of EPR assumed by the metallic part under test (which is supposed leaking a unitary current) that is transferred on the ground electrode of the considered substation. So it can be deduced that $0 \leq \beta < 1$. Moreover, with reference to eq. (2), it must be $\beta R_{BC} < 1 \cdot R_{ES}$. Taking into account that R_{BC} resistance must be positive, it is possible to write the following inequalities set:

$$\begin{cases} 0 \leq \beta < 1 \\ \beta R_{BC} < 1 \cdot R_{ES} \\ R_{BC} > 0 \end{cases} \tag{10}$$

The solution of eq. set (10) identifies two different ranges of R_{BC} values as a function of K.

$$R_{BC} \in \begin{cases} \left[(K-1)\,R_{ES}, (K+1)\,R_{ES}\right], & K \geq 1 \\ \left[(1-K)\,R_{ES}, (K+1)\,R_{ES}\right], & K < 1 \end{cases} \tag{11}$$

So, for each measured value of K, it is possible to evaluate the minimum and maximum value of R_{BC}. The more the inequalities (12) are true, the smaller is the R_{BC} range in (11).

$$K << 1 \quad or \quad K >> 1 \tag{12}$$

An application example of the method to compute the minimum and the maximum values of R_{BC} is now provided. The considered scenario is reported in Fig. 15: a square electrode (ES) and an earthing rod (BC) are buried at 0.5 m under the soil surface. Geometrical details are reported in Table II. The scenario was modeled through the Maxwell's Subareas Method (MaSM) [7]. The resistances R_{ES} and R_S were computed and reported in Table III. The K ratio, evaluated according to eq. (7), is equal to 13.7.

From the set of equations (11), the minimum and maximum values of R_{BC} were calculated. Their values are respectively 66.2 Ω and 76.6 Ω.

In order to verify the range, the "true" value of R_{BC} was then computed. It is equal to 72.1 Ω. As expected, it is in the forecasted range.

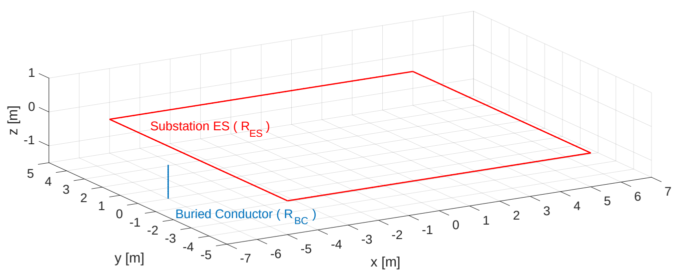

Figure 15. Example of application: considered layout..

Table II
Example of Application: Geometrical Details

Quantity	Values
Length of square ES	10 m
Length of the earthing rod BC	1 m
Distance between ES and R_{BC}	1 m
Cross section of ES and BC electrodes	9 mm
Soil resistivity	100 Ωm

Table III
EXAMPLE OF APPLICATION: RESULTS

Quantity	Values
R_{ES}	5.2Ω
R_S	71.4Ω
K	13.7
Min R_{BC}	66.2Ω
Max R_{BC}	76.6Ω

REFERENCES

[1] E. Pons, P. Colella, R. Napoli, and R. Tommasini, "Impact of MV ground fault current distribution on global earthing systems," *Industry Applications, IEEE Transactions on*, vol. 51, no. 6, pp. 4961–4968, 2015.

[2] A. Campoccia, E. R. Sanseverino, and G. Zizzo, "Analysis of interconnected earthing systems of MV/LV substations in urban areas," in *Universities Power Engineering Conference, 2008. UPEC 2008. 43rd International*. IEEE, 2008, pp. 1–5.

[3] R. Tommasini, R. Pertusio, and S. Toja, "FEM approach to the study of global earthing systems," in *International Association of Science and Technology for Development (IASTED), 2003 3rd International Conference on*, 2003, pp. 737–740.

[4] P. Colella, R. Napoli, E. Pons, R. Tommasini, A. Barresi, G. Cafaro, A. De Simone, M. L. Di Silvestre, L. Martirano, P. Montegiglio, E. Morozova, G. Parise, L. Parise, E. Riva Sanseverino, F. Torelli, F. Tummolillo, G. Valtorta, and G. Zizzo, "Currents distribution during a fault in an MV network: Methods and measurements," *IEEE Transactions on Industry Applications*, vol. 52, no. 6, pp. 4585–4593, Nov 2016.

[5] P. Colella, R. Napoli, E. Pons, R. Tommasini, A. Barresi, G. Cafaro, A. De Simone, M. Di Silvestre, L. Martirano, P. Montegiglio *et al.*, "Current and voltage behaviour during a fault in a HV/MV system: Methods and measurements," in *Environment and Electrical Engineering (EEEIC), 2015 IEEE 15th International Conference on*. IEEE, 2015, pp. 404–409.

[6] G. Parise, L. Parise, and L. Martirano, "Identification of global grounding systems: the global zone of influence," *Industry Applications, IEEE Transactions on*, vol. 51, no. 6, pp. 5044–5049, 2015.

[7] E. Pons, P. Colella, R. Tommasini, R. Napoli, P. Montegiglio, G. Cafaro, and F. Torelli, "Global earthing system: can buried metallic structures significantly modify the ground potential profile?" *Industry Applications, IEEE Transactions on*, vol. 51, no. 6, pp. 5237–5246, 2015.

[8] G. Parise, L. Martirano, L. Parise, F. Tummolillo, G. Vagnati, A. Barresi, G. Cafaro, P. Colella, M. L. Di Silvestre, P. Montegiglio, E. Morozova, R. Napoli, E. Pons, E. Riva Sanseverino, S. Sassoli, R. Tommasini, F. Torelli, G. Valtorta, and G. Zizzo, "A practical method to test the safety of HV/MV substation grounding systems," in *2015 IEEE 15th International Conference on Environment and Electrical Engineering (EEEIC)*. IEEE, June 2015, pp. 502–506.

[9] *Power installations exceeding 1 kV a.c., Part 1: Common rules*. IEC EN 61936-1, 07 2011.

[10] *Earthing of power installations exceeding 1 kV a.c.* CEI EN 50522, 07 2011.

[11] G. Cafaro, P. Montegiglio, F. Torelli, P. Colella, R. Napoli, E. Pons, R. Tommasini, A. De Simone, E. Morozova, G. Valtorta, A. Barresi, F. Tummolillo, A. Campoccia, M. L. Di Silvestre, E. Riva Sanseverino, G. Zizzo, L. Martirano, G. Parise, and L. Parise, "The global grounding system: Definitions and guidelines," in *2015 IEEE 15th International Conference on Environment and Electrical Engineering (EEEIC)*. IEEE, June 2015, pp. 537–541.

[12] P. Colella, E. Pons, and R. Tommasini, "A comparative review of the methodologies to identify a global earthing system," *IEEE Transactions on Industry Applications*, vol. 53, no. 4, pp. 3260–3267, July 2017.

[13] ——, "The identification of global earthing systems: a review and comparison of methodologies," 2016, Environment and Electrical Engineering (EEEIC), 2016 IEEE 16th International Conference on.

[14] G. Parise, L. Parise, and L. Martirano, "Single grounding system intrinsically safe and global grounding system safe as set," Environment and Electrical Engineering (EEEIC), 2016 IEEE 16th International Conference on.

[15] M. L. Di Silvestre, L. Dusunchet, S. Mangione, and G. Zizzo, "On the effects of HV/MV stations on global grounding systems," 2016, Environment and Electrical Engineering (EEEIC), 2016 IEEE 16th International Conference on.

[16] M. Desmedt, J. Hoeffelman, and D. Halkin, "Use of a global earthing system to implement the safety requirements for protecting against indirect contacts in HV systems," in *Electricity Distribution, 2001. Part 1: Contributions. CIRED. 16th International Conference and Exhibition on (IEE Conf. Publ No. 482)*, vol. 2. IET, 2001, pp. 10–14.

[17] L. Fickert, E. Schmautzer, C. Raunig, and M. J. Lindinger, "Verification of global earthing systems," in *Electricity Distribution (CIRED 2013), 22nd International Conference and Exhibition on*, 2013, pp. 1–4.

[18] G. Cafaro, P. Montegiglio, F. Torelli, A. Barresi, P. Colella, A. De Simone, M. L. Di Silvestre, L. Martirano, E. Morozova, R. Napoli, G. Parise, L. Parise, E. Pons, E. Riva Sanseverino, R. Tommasini, F. Tummolillo, G. Valtorta, and G. Zizzo, "Influence of LV neutral grounding on global earthing systems," *IEEE Transactions on Industry Applications*, vol. 53, no. 1, pp. 22–31, Jan 2017.

[19] *Low-voltage electrical installations - Part 4-41*. IEC 60364-4-41, 12 2005.

[20] G. Cafaro, P. Montegiglio, F. Torelli, P. Colella, E. Pons, R. Tommasini, and G. Valtorta, "Global earthing systems: Characterization of buried metallic parts," in *2016 IEEE 16th International Conference on Environment and Electrical Engineering (EEEIC)*. IEEE, June 2016, pp. 1–6.

[21] V. Cataliotti and A. Campoccia, *Impianti di terra*. TNE, 2013.

[22] F. Freschi, M. Mitolo, and M. Tartaglia, "Interferences phenomena between separate grounding systems," *IEEE Transactions on Industry Applications*, vol. 50, no. 4, pp. 2853–2860, 2014.

[23] R. Gustafson, R. Pursley, and V. Albertson, "Seasonal grounding resistance variations on distribution systems," *Power Delivery, IEEE Transactions on*, vol. 5, no. 2, pp. 1013–1018, 1990.

[24] J. He, R. Zeng, Y. Gao, Y. Tu, W. Sun, J. Zou, and Z. Guan, "Seasonal influences on safety of substation grounding system," *IEEE Transactions on Power Delivery*, vol. 18, no. 3, pp. 788–795, 2003.

[25] M. Unde and B. Kushare, "Impact of seasonal variation of soil resistivity on safety of substation grounding system," 2013.

[26] *IEEE Guide for Safety in AC Substation Grounding*. IEEE Standard 80, 01 2000.